Georgia Tech Sponsored Research

45

Project	E-20-671 3266
Project director	Kapoor Vivek
Research unit	CEE
Title	Coupling Chemical Transformation Kinetics & Subsurface Transport
Project date	9/30/2001

E-20-671

Final Report for Period: 07/1998 - 06/2001 **Submitted on:** 07/24/2001

Principal Investigator: Kapoor, Vivek . **Award ID:** 9803663

Organization: GA Tech Res Corp - GIT

Title:

Coupling Chemical Transformation Kinetics and Subsurface Transport

Project Participants

Senior Personnel

Name: Kapoor, Vivek

Worked for more than 160 Hours: Yes

Contribution to Project:

Post-doc

Graduate Student

Name: Felton, Scott

Worked for more than 160 Hours: Yes

Contribution to Project:

Scott Felton is analyzing the implications of bimolecular reaction kinetics on dissolution processes.

Name: Anmala, Jagadeesh

Worked for more than 160 Hours: Yes

Contribution to Project:

Jagadeesh is exploring a theoretical and modeling framework to represent chemical kinetics at scales of hydrologic interest.

Undergraduate Student

Research Experience for Undergraduates

Organizational Partners

Other Collaborators or Contacts

Note: Dr. Kapoor is no longer employed by Georgia Tech and has no contact with the Institute. The final report was submitted by Dr. Donald Webster to the best of his information and knowledge of the project.

Professor Dennis A Lyn, an experimental fluid mechanician, and Professor Chad T. Jafvert, an environmental geochemist have been collaborators on the experimental part of this project.

Activities and Findings

Project Activities and Findings:

EXPERIMENTS

The experimental findings of the influence of reactant segregation in porous media have been communicated to the journal Env. Sci. and Tech.

THEORETICAL AND NUMERICAL

An analytical dissolution rate coefficient that is independent of

Project Training and Development:
THEORETICAL AND NUMERICAL

1. The macroscopic dispersive flux of solutes undergoing aqueous phase bimolecular reactions can be described in the same manner as that of a non-reactive solute. In a linear gradient dependent relationship for the macrodispersive flux the macrodispersion coefficient remains unchanged on account of transformation reactions.

2. The concentration variance and the cross-covariance between the reactant concentrations also undergo a macrodispersive flux that can be described using a linear gradient relationship with the macrodispersion coefficient being the same as that for the mean dispersive flux of a non-reactive solute.

3. The dominant balance in the cross-covariance budget is between its rates of production and dissipation of concentration cross-covariance, with, and without reactions. The same balance holds for the concentration variances.

4. The characteristic time-scale over which small-scale mixing (local dispersion) dissipates the concentration variance and the cross-covariance, which we refer to as the ôdissipation time scale,ö and has been previously referred to as the ôvariance residence time,ö is unaffected by reaction.

5. The macrodispersion coefficient and the dissipation time scale appear to approach constant asymptotic values, although the dissipation time scale approaches that asymptotic constant level much slower than the macrodispersion coefficient.

6. Exploiting the dominant production dissipation balance in the concentration cross-covariance budget yields a simple formula for the concentration cross covariance. The macrodispersion coefficients, the dissipation time-scale, and the product of the mean reactant concentration gradients control the reactant concentration cross-covariance. The influence of the flow microstructure and small-scale mixing are present in this model through the macrodispersion coefficient and the dissipation time-scale. This formula for the concentration cross-covariance was shown to apply under reactive and non-reactive conditions.

7. The simple result for the concentration cross-covariance that reflects the production-dissipation balance that characterizes second order fluctuation budgets can be applied to upscale bimolecular reactions and results in a macroscopic gradient dependent effective rate parameter. The effective rate parameter can be larger than its intrinsic value (inferred under well-mixed conditions) if the macroscopic gradients have identical signs (initially overlapping case) or smaller than the intrinsic value if the macroscopic gradients have opposite signs (initially non-overlapping reactants). The effective reaction rate parameter for the bimolecular reaction derived here provides a specific example of how mixing in a heterogeneous environment controls the reaction rates. The macro-kinetics themselves are dependent on the macroscopic concentration gradient, because these gradients control the small-scale concentration fluctuations of the reactants. It is easy to incorporate the gradient dependent reaction macro-kinetics in models that routinely evaluate the mean concentration field and its gradients.

8. The upscaling of dual-Monod kinetics expression - that is widely used to model biodegradation kinetics - is illustrated based on the expressions for concentration covariance and variances developed in this work. It is shown how reactant segregation can appreciably slow down the attenuation rate of an aerobically biodegradable contaminant.

9. An analytical dissolution rate coefficient that is independent of scale was developed in order to yield more realistic models for mass transfer in rock fractures. The analytical solution yields the mean velocity, dispersion coefficient and dissolution rate coefficient, which are independent of scale and may be applied to NAPL and solid dissolution.

Research Training:
D. Scott Felton finished his MS thesis in December 2000.

Jagadeesh Anmala finished his PhD dissertation in August 2000.

Outreach Activities:
CHAPMAN CONFERENCE PROPOSAL
Based on the positive feedback we have received from a broad range of researchers Kapoor have initiated the process for organizing a Chapman Conference on the topic of this proposal.

CONFERENCE PRESENTATIONS
Anmala, J., V. Kapoor, Mixing and bimolecular reaction kinetics in stratified flows, EOS Trans. AGU, 80(46), F414-F415, 1999.

Kapoor, V., J. Anmala, Chemical transformation kinetics in subsurface flows, EOS Trans. AGU, 80(17), S156, 1999.

Journal Publications

D. Raje and V. Kapoor

, "Experimental study of a bimolecular reaction in Porous Media", Env. Sci. Tech, p. 1234, vol. 34, (2000). Published

J. Anmala, V. Kapoor, "Dynamics of mixing and kinetics of bimolecular reactions aquifers", Water Resour Res, p. , vol. , (2001). Submitted

Books or Other One-time Publications

V. Kapoor, P. K. Kitanidis, "Concentration fluctuations, dilution, and risk assessment: The role of local dispersion and heterogeneity", (2000).
Book, Accepted
Editor(s): G. S. Govindaraju
Collection: Stochastic Methods in Subsurface Contaminant Hydrology
Bibliography: to appear

Web/Internet Site

URL(s):

Description:

Other Specific Products

Contributions

Contributions within Discipline:

Kinetics of chemical transformations and dynamics of mixing in subsurface flows:

To quantify chemical transformations in natural hydrologic environments the coupling of transformation kinetics with flows was described in this work. Flow microstructure and small-scale mixing were shown to control the segregation of reactants, and therefore also determine the macroscopic reaction kinetics for multi-species nonlinear reactive transport. The rates of attenuation of a pollutant, due to chemical transformations reactions associated with the interaction of the pollutant and other species in the aqueous subsurface environment, i.e., the reaction macro-kinetics, were shown to depend on the macroscopic spatial gradients of the reactants. In addition to numerical simulations and theoretical analysis that lead to new expressions for reaction macro-kinetics, a bimolecular chemical reaction was experimentally studied to document the flow heterogeneity and incomplete mixing induced scale-dependent transformation kinetics.

Contributions to Other Disciplines:

The project is on the interdisciplinary topic of chemical transformation kinetics in flows, and the progress is at the interface of two disciplines.

Contributions to Human Resource Development:

1 PhD thesis completed (Aug 2000)
1 MS thesis completed (Dec 2000)

Contributions to Science and Technology Infrastructure:

Experimental to observe reactive transport developed iun this project is used to teach undergraduates a course on 'Environmental Transport Processes.'

Contributions: Beyond Science or Engineering:

Categories for which nothing is reported:

Organizational Partners

Any Product

Contributions: Beyond Science or Engineering

TABLE OF CONTENTS

CHAPTER I

INTRODUCTION

Fractures in native rock are a problem because dissolved contaminants can leach into a fracture and diffuse into the surrounding walls. Furthermore, as water flows through a fracture, the walls can dissolve over time. The dissolved minerals can precipitate, coating the fracture walls, which affects the sorption of contaminants onto the walls. These contaminants become trapped in the rock matrix, which makes remediation difficult. Understanding and modeling these flows is difficult for several reasons including the challenge of distinguishing between kinetics due to mass transfer of contaminants and those intrinsic to the dissolution of the rock fracture. This study develops a theoretical mass transfer rate for dissolution of rock fractures by analytically solving the two-dimensional (2D) advection-dispersion equation.

Dissolution has been studied extensively using physical experiments and computational simulations. The dissolution of rock fractures can be predicted by assuming a first-order irreversible kinetic surface reaction in the advection-diffusion equation and using Taylor (1953) type approximations to obtain the dimensionless mean concentration (Dijk and Berkowitz, 1998). Assuming a first order reaction requires that the reaction rate to be known a priori, again preventing generality between the laboratory and field.

The objective of this study is to develop an analytical dissolution rate coefficient, independent of scale. Ultimately, the coefficient should yield more realistic models for describing mass transfer in rock fractures. Following the analysis of Taylor (1953), a 2D laminar shear flow solution is found for the flow between parallel plates, where the mass transfer of a solute in the aqueous phase will be specified at the fixed wall boundaries. This idealized flow simulates flow in a rock fracture with dissolving walls. The analytical solution yields a mean velocity, dispersion coefficient and a dissolution rate coefficient, which are independent of scale and may be applied to NAPL or solid dissolution based on similar physical mechanisms. To validate the analytical solution, the diffusive flux, concentration gradient in the transverse direction, and mean concentration are compared to the results of numerical simulations of the 2D advection-dispersion equation using a central finite difference method.

CHAPTER II

LITERATURE REVIEW

The physical, chemical, and biological processes that control dissolution reaction kinetics in aquatic systems are often poorly understood, scale-dependent, and difficult to describe by theoretical mathematics. In order to make an accurate prediction of dissolution rate coefficients at the field-scale, the macroscopic processes of advection and dispersion, must be taken into account. Four basic processes are important for transfer of solutes from a solid surface to the aqueous phase: diffusion in the solution boundary layer adjacent to the surface, sorption on the solid surface, migration on the surface to or from a step edge, and migration along a step edge to or from a surface discontinuity. The work presented herein, will focus on diffusion-controlled dissolution, which is analogous to gas transfer at the air-water interface by molecular diffusion of solutes across a boundary layer whose thickness is defined by the fluid mechanics of the flow (Morel, 1983).

In this chapter, literature describing solute and radionuclide dissolution in rock fractures, and Taylor dispersion are presented. The purpose is to provide background material necessary to develop the mathematical analysis described in this thesis.

2.1 Solute Dissolution in Rock Fractures

For the specific case of a rock fracture, dissolution can affect the physical and chemical properties of the fracture media. In this context, dissolution refers to the mass transfer of a solute or radionuclide from the fracture walls into the aqueous phase.

Dijk and Berkowitz (1998) evaluated the dissolution and precipitation of reactive solutes in rock fractures and the effect of initial fracture geometry and the solute saturation content on reaction processes. The idealized fracture system was defined as the gap between two infinite parallel plates. The fluid density and viscosity were assumed to be constant, and a fully developed parabolic laminar velocity profile was assumed. The dissolution and precipitation were described as a first-order irreversible kinetic surface reaction, given as

$$\frac{\partial C}{\partial t} = k(C_{sat} - C) \tag{2-1}$$

where k is the reaction rate constant [t^{-1}], C_{sat} is the saturation concentration [ML^{-3}], and C is the solute concentration at the wall [ML^{-3}]. The values for the rate coefficient k and saturation concentration C_{sat} were taken from available literature describing the precipitation of quartz. Because the values reported by Dijk and Berkowitz (1998) were obtained through laboratory experiments, the analysis lacks generality between laboratory and field scales. In order to solve the transport equation, Dijk and Berkowitz (1998) employed a finite difference scheme to numerically solve the equation for a range of velocities. Dijk and Berkowitz (1998) using the approach of Taylor (1953) developed an expression for the mean concentration. A constant concentration was specified at the

inlet and a zero-gradient concentration profile was specified at the outlet. The wall boundary condition was a mass balance for the solute deposition and dissolution with an initial quasi-steady state condition, which states that the deposition and dissolution directly affect the wall aperture.

Bekri et al. (1997) developed a numerical solution for dissolution and deposition-dissolution cycles in rock fractures based on Taylor dispersion. In their approach, the fracture geometry changed over time, which affected the flow profile in the fracture. The Stokes equation was solved to determine the varying flow profile. Once the velocity profile was known, the transport equation was solved using a finite difference scheme for a range of velocities and reaction rates where the boundary condition applied at the wall surface was a first-order reaction (Equation 2-1).

Parker et al. (1994) performed experiments to investigate the disappearance times of dense non-aqueous phase liquids (DNAPLs) in rock fractures. The conceptual model consisted of DNAPL in the dissolved phase within a fracture diffusing into the surrounding rock matrix. The authors modeled chemical mass flux from the fracture surface into the rock matrix as a Fickian diffusion process:

$$J_D = -\theta D_e \frac{\partial C}{\partial x} \tag{2-2}$$

where J_D is the diffusive flux [$ML^{-2}t^{-1}$], θ is the matrix porosity, and D_e is the effective diffusion coefficient [L^2t^{-1}]. The wall concentration of the fracture was assumed to be equal to the aqueous solubility of the chemical. Although the model used by Parker et al.

(1994) was applied to a solute diffusing into the rock matrix from a fracture surface, the reverse process can be modeled in a similar fashion.

Holtta et al. (1996) investigated the effects of matrix diffusion on radionuclides in rock fractures. The matrix diffusion and hydrodynamic dispersion were measured for tritiated water and chloride transport in both mica gneiss and tonalite columns. Holtta et al. (1996) calculated the advection and hydrodynamic dispersion using a numerical compartment model that can account for both Fickian and non-Fickian processes. Again, while the experiment studied diffusion of radionuclides into rock fractures, the reverse process can be modeled similarly.

2.2 Taylor Dispersion

Dispersive transport results from physical phenomena at different scales, such as fluid advection and molecular diffusion. In the case of porous media, dispersion results from the disruption of flow lines by obstacles or surfaces. In a given time period, solute traveling on a direct path moves much farther than solute encountering significant blockage. Hence, the solute spreads in the direction of flow and decreases in concentration (Weber and DiGiano, 1996).

In the context of soluble salts in the blood stream, Taylor (1953) investigated the dispersion of solutes flowing through a tube with a parabolic velocity profile. Taylor (1953) showed that a dispersion coefficient could be explicitly calculated from the known properties of the flow field and the diffusivity of the solute. Taylor dispersion occurs in shear flows due to uneven advective transport and molecular diffusion. In a shear layer,

faster flow transports a passive solute farther within a given time interval, thus creating a concentration gradient in the transverse direction. Molecular diffusion of the solute then acts in the transverse direction to homogenize the distribution. The Taylor dispersion coefficient is an inverse function of the molecular diffusion coefficient. Thus, rapid diffusion leads to small dispersion and slow diffusion produces large dispersion.

The pressure-driven velocity profile between parallel plates is also parabolic, thus the dispersion effects are similar to the tube geometry addressed by Taylor (1953). Following the analysis of Taylor (1953) and Aris (1956) for the simple case of a nonreactive solute and a parabolic flow profile between two parallel plates (Figure 2-1),

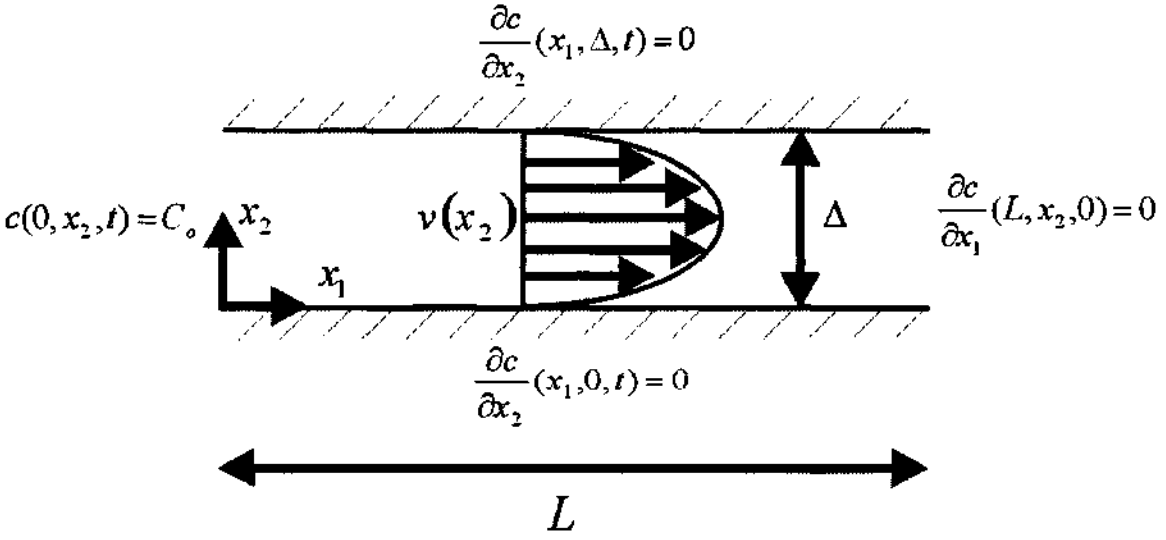

Figure 2-1 Definition Sketch

the transport equation can be written:

$$\frac{\partial c}{\partial t} + v(x_2)\frac{\partial c}{\partial x_1} - d\left[\frac{\partial^2 c}{\partial x_1^2} + \frac{\partial^2 c}{\partial x_2^2}\right] = 0 \qquad (2\text{-}3)$$

where c is the concentration of a solute [ML^{-3}], d is the diffusivity [L^2t^{-1}], x_1 is the flow direction [L], and x_2 is the transverse direction. The velocity profile $v(x_2)$ is

$$v(x_2) = V\left[6\frac{x_2}{\blacksquare} - 6\frac{x_2^2}{\blacksquare^2}\right] \tag{2-4}$$

where V is the mean velocity [Lt^{-1}] and λ is the distance between the plates [L]. The boundary conditions for the solute concentration are specified as zero flux at the walls:

$$\frac{\blacksquare c}{\blacksquare x_2}(x_1, 0, t) = 0 \qquad 0 < x_1 < L;$$

$$\frac{\blacksquare c}{\blacksquare x_2}(x_1, \blacksquare, t) = 0 \qquad 0 < x_1 < L;$$

concentration C_o at the inlet:

$$c(0, x_2, t) = C_o \qquad 0 < x_2 < \blacksquare;$$

and zero longitudinal gradient at the outlet:

$$\frac{\blacksquare c}{\blacksquare x_1}(L, x_2, t) = 0 \qquad 0 < x_2 < \blacksquare.$$

The initial condition is zero concentration everywhere:

$$c(x_1, x_2, 0) = 0 \qquad 0 < x_1 < L,\ 0 < x_2 < \blacksquare.$$

To account for fluctuations in the flow, the velocity and concentration are decomposed into cross-sectional mean and fluctuation:

$$c = C + c'; \qquad v = V + v',$$

and substituting into the 2D transport equation (2-3) gives:

$$\frac{\blacksquare C}{\blacksquare t} + \frac{\blacksquare c'}{\blacksquare t} + V\frac{\blacksquare C}{\blacksquare x_1} + V\frac{\blacksquare c'}{\blacksquare x_1} + v'\frac{\blacksquare C}{\blacksquare x_1} + v'\frac{\blacksquare c'}{\blacksquare x_1} - d\left[\frac{\blacksquare^2 C}{\blacksquare x_1^2} + \frac{\blacksquare^2 c'}{\blacksquare x_1^2} + \frac{\blacksquare^2 C}{\blacksquare x_2^2} + \frac{\blacksquare^2 c'}{\blacksquare x_2^2}\right] = 0$$

(2-5)

Averaging each term of (2-5) in the x_2 direction (where averaging of a quantity q is defined as $\bar{q} = \frac{1}{\Delta}\int_0^{\Delta} q(x_2)dx_2$), causes the derivatives with respect to the x_2 direction to drop out. Realizing that the mean of a fluctuation is zero by definition, and applying continuity:

$$\frac{\partial C}{\partial t} + V\frac{\partial C}{\partial x_1} + \frac{\partial \overline{c'v'}}{\partial x_1} - d\frac{\partial^2 C}{\partial x_1^2} = 0 \tag{2-6}$$

The term $\frac{\partial \overline{c'v'}}{\partial x_1}$ is the gradient of the mean of the product of concentration and velocity fluctuations and physically corresponds to the transport due to fluctuations. The objective of this analysis is to produce an analytical model for this term. Subtracting (2-6) from (2-5), and then linearizing:

$$\frac{\partial c'}{\partial t} + V\frac{\partial c'}{\partial x_1} - d\left[\frac{\partial^2 c'}{\partial x_1^2} + \frac{\partial^2 c'}{\partial x_2^2}\right] = -v'\frac{\partial C}{\partial x_1} \tag{2-7}$$

Assuming that longitudinal diffusion is much smaller than transverse diffusion, (2-7) can be rewritten:

$$\frac{\partial c'}{\partial t} + V\frac{\partial c'}{\partial x_1} - d\frac{\partial^2 c'}{\partial x_2^2} = -v'\frac{\partial C}{\partial x_1} \tag{2-8}$$

For steady-state with small variation of the concentration fluctuation in the longitudinal direction, (2-8) reduces to:

$$-d\frac{\partial^2 c'}{\partial x_2^2} = -v'\frac{\partial C}{\partial x_1} \tag{2-9}$$

Because diffusive transport dominates advective transport at with respect to time steady-state, the mean velocity V is assumed negligible compared to the velocity fluctuation v'. Solving (2-4) in terms of v' (i.e. $v' = v(x_2) - V$), and integrating (2-9) twice with respect to x_2 gives the zero-mean solution:

$$c' = \frac{V}{d}\frac{\partial C}{\partial x_1}\left[\frac{x_2^3}{\alpha} - \frac{x_2^4}{2\alpha^2} - \frac{x_2^2}{2}\right] \tag{2-10}$$

multiplying both sides with v', and averaging along the x_2 direction gives the diffusive flux:

$$\overline{c'v'} = -\frac{V^2\alpha^2}{210d}\frac{\partial C}{\partial x_1} \tag{2-11}$$

Differentiating (2-11), and substituting into (2-6), and assuming that longitudinal diffusion is much smaller than dispersion, the transport equation for the mean concentration is obtained:

$$\frac{\partial C}{\partial t} + V\frac{\partial C}{\partial x_1} - D^*\frac{\partial^2 C}{\partial x_1^2} = 0 \tag{2-12}$$

Where the Taylor dispersion for the mean transport equation is:

$$D^* = d + \frac{V^2\alpha^2}{210d} \tag{2-13}$$

Which is the Taylor dispersion coefficient for a parallel-plate fracture [e.g. Fischer et al., 1979] that provides a means to predict the transport of a solute that is independent of scale.

2.3 Objectives of Study

The objective of this study is to predict the dissolution rate of a solute in a rock fracture. An analytical approach similar to that of Taylor (1953) and Aris (1956) will be applied to a parallel plate fracture with a parabolic velocity profile in order to develop a mean transport equation that is independent of scale. Following the rock fracture models utilized by Dijk and Berkowitz (1998), Parker et al. (1994), and Holtta et al. (1996), mass transfer of a solute in the aqueous phase will be specified at the walls. The resulting rate coefficient will be independent of scale and thus applicable at both laboratory and field scales unlike the rate coefficients used by Dijk and Berkowitz (1998) which were taken from available literature and only applicable to the laboratory scale.

CHAPTER III

METHODOLOGY

An analytical solution for the dissolution rate coefficient is found using the analysis of Taylor (1953) and Aris (1956) for a 2D laminar shear flow between parallel plates (Section 2.2). In the current work, the solute concentration in the aqueous phase at the wall boundaries is specified as a constant rather than zero, thus representing dissolution of a solute at the walls. The analytical solution to the 2D transport equation produces a mean velocity, dispersion coefficient, and dissolution rate coefficient that are independent of scale. Furthermore, the diffusive flux, concentration gradient in the transverse direction, and the mean concentration are solved via numerical simulation to validate the analytical solution.

3.1 Dimensional Analysis

The advective and diffusive transport mechanisms acting on the solute can be characterized by the dimensionless Peclet number:

$$Pe = \frac{V\blacksquare}{d} \tag{3-1}$$

which describes the effect of advection relative to molecular diffusion. By replacing each term in the 2D transport equation (2-3) with corresponding dimensionless terms, the

analytical and numerical solutions will yield results that are scale independent. Choosing the characteristic length, velocity and concentration as the gap dimension, mean velocity, and wall concentration, respectively, the dimensionless coordinates follow:

$$x_1^* = \frac{x_1}{\blacksquare} \qquad x_2^* = \frac{x_2}{\blacksquare} \qquad t^* = \frac{tV}{\blacksquare} \tag{3-2}$$

and the dimensionless velocity and concentration:

$$v^* = \frac{v}{V} \qquad c^* = \frac{c}{C_w} \tag{3-3}$$

Substituting into the 2D transport equation (2-3):

$$\frac{\blacksquare c^*}{\blacksquare t^*} \blacksquare v^* \frac{\blacksquare c^*}{\blacksquare x_1^*} - \frac{1}{Pe}\left[\frac{\blacksquare^2 c^*}{\blacksquare x_1^{*2}} \blacksquare \frac{\blacksquare^2 c^*}{\blacksquare x_2^{*2}}\right] = 0 \tag{3-4}$$

From this non-dimensional equation, the relative importance of the advection and diffusion can be ascertained. For Pe = 1 the advection and diffusion terms are of the same order. For Pe > 1 advection dominates, while Pe < 1 diffusion dominates.

3.2 Analytical Approach

The basic analytical approach described in Section 2.2 is followed to obtain the solution for flow between parallel plates. The wall boundaries are at a fixed location with a specified concentration as sketched in Figure 3-1. The current arrangement also differs from that of Taylor (1953) because the inflow concentration is zero. Physically, this corresponds to clean fluid flowing through a rock fracture while entraining solute from

the walls. The Reynolds number for the results presented in the next chapter are in the range of 0.0005 to 5 which are, indeed, in the laminar regime.

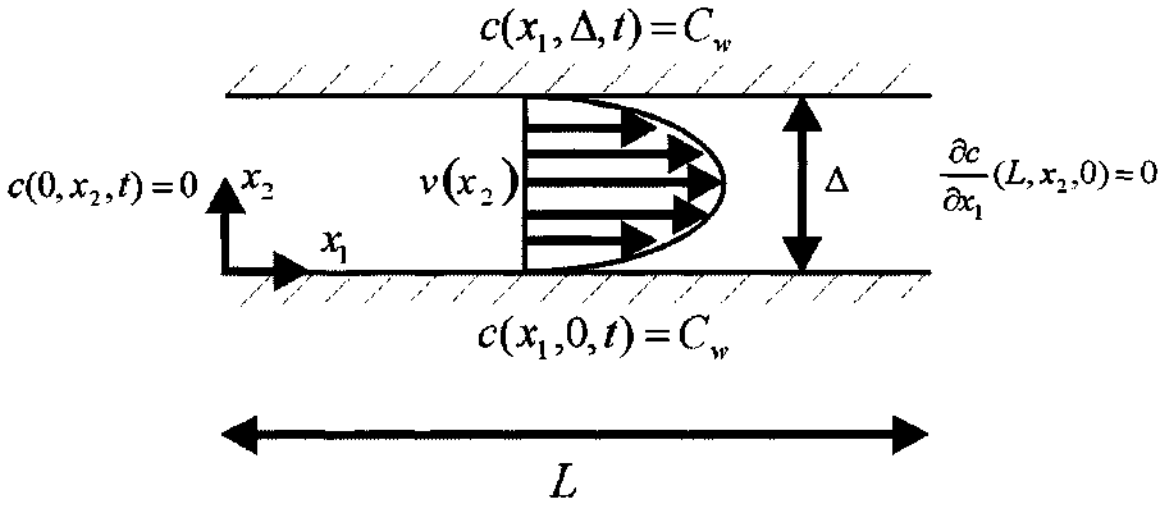

Figure 3-1 Definition Sketch

The transport equation can be written:

$$\frac{\partial c}{\partial t} + v(x_2)\frac{\partial c}{\partial x_1} - d\left[\frac{\partial^2 c}{\partial x_1^2} + \frac{\partial^2 c}{\partial x_2^2}\right] = 0 \tag{3-5}$$

where c is the concentration of a solute, d is the diffusivity of the solute in the fluid, x_1 is the flow direction, and x_2 is the transverse direction. The velocity profile $v(x_2)$ is

$$v(x_2) = V\left[6\frac{x_2}{\lambda} - 6\frac{x_2^2}{\lambda^2}\right] \tag{3-6}$$

where V is the mean velocity and λ is the distance between the plates. The boundary conditions at the walls are equal to a constant wall concentration, C_w:

$c(x_1, 0, t) = C_w \qquad 0 < x_1 < L;$

$c(x_1, \blacksquare, t) = C_w \qquad 0< x_1<L;$

zero concentration at the inlet:

$c(0, x_2, t) = 0 \qquad 0< x_2<\blacksquare;$

and zero longitudinal gradient at the outlet:

$$\frac{\partial c}{\partial x_1}(L, x_2, t) = 0 \qquad 0< x_2<\blacksquare.$$

The initial condition is zero concentration everywhere:

$c(x_1, x_2, 0) = 0 \qquad 0< x_1<L,\ 0< x_2<\blacksquare.$

To account for turbulent fluctuations in the flow, the velocity and concentration are decomposed into cross-sectional mean and fluctuation:

$c = C + c'; \qquad v = V + v'.$

Substituting into the 2D transport equation (3-5) gives:

$$\frac{\partial C}{\partial t} + \frac{\partial c'}{\partial t} + V\frac{\partial C}{\partial x_1} + V\frac{\partial c'}{\partial x_1} + v'\frac{\partial C}{\partial x_1} + v'\frac{\partial c'}{\partial x_1} - d\left[\frac{\partial^2 C}{\partial x_1^2} + \frac{\partial^2 c'}{\partial x_1^2} + \frac{\partial^2 C}{\partial x_2^2} + \frac{\partial^2 c'}{\partial x_2^2}\right] = 0 \qquad (3\text{-}7)$$

Averaging each term of (3-7) in the x_2 direction causes the derivatives with respect to the x_2 direction to drop out. Realizing that the mean of a fluctuation is zero by definition and applying continuity:

$$\frac{\partial C}{\partial t} + V\frac{\partial C}{\partial x_1} + \frac{\partial \overline{c'v'}}{\partial x_1} - d\frac{\partial^2 C}{\partial x_1^2} = -\frac{d}{\blacksquare}\left[\frac{\partial c'}{\partial x_2}\Big|_{\blacksquare} - \frac{\partial c'}{\partial x_2}\Big|_{0}\right] \qquad (3\text{-}8)$$

The term $\frac{\partial \overline{c'v'}}{\partial x_1}$ is the gradient of the mean of the product of concentration and velocity fluctuations and physically corresponds to the transport of solute due to fluctuations. The objective of this analysis is to produce an analytical model for this term.

Subtracting (3-8) from (3-7) and then linearizing:

$$\frac{\partial c'}{\partial t} + V\frac{\partial c'}{\partial x_1} - d\left[\frac{\partial^2 c'}{\partial x_1^2} + \frac{\partial^2 c'}{\partial x_2^2}\right] = -v'\frac{\partial C}{\partial x_1} - \frac{d}{\varepsilon}\left[\frac{\partial c'}{\partial x_2}\Big|_0\right] \tag{3-9}$$

Assuming longitudinal diffusion is much smaller than transverse diffusion:

$$\frac{\partial c'}{\partial t} + V\frac{\partial c'}{\partial x_1} - d\frac{\partial^2 c'}{\partial x_2^2} = -v'\frac{\partial C}{\partial x_1} - \frac{d}{\varepsilon}\left[\frac{\partial c'}{\partial x_2}\Big|_0\right] \tag{3-10}$$

For steady-state with mild variation of the concentration fluctuation in the longitudinal direction, (3-10) reduces to:

$$-d\frac{\partial^2 c'}{\partial x_2^2} = -v'\frac{\partial C}{\partial x_1} - \frac{d}{\varepsilon}\left[\frac{\partial c'}{\partial x_2}\Big|_0\right] \tag{3-11}$$

Reformulating (3-6) in terms of v' (i.e. $v' = v(x_2) - V$), substituting into (3-11) and integrating twice with respect to x_2 gives the zero-mean solution:

$$dc'(x_2) - d(C_w - C) = V\left[\frac{x_2^3}{3\varepsilon} - \frac{x_2^4}{2\varepsilon^2} - \frac{x_2^2}{2}\right]\frac{\partial C}{\partial x_1} + \frac{dx_2^2}{2\varepsilon}\left[\frac{\partial c'}{\partial x_2}\Big|_\lambda\right] - \left[dx_2 - \frac{dx_2^2}{2\varepsilon}\right]\left[\frac{\partial c'}{\partial x_2}\Big|_0\right] \tag{3-12}$$

Evaluating this expression at the wall ($x_2 = \lambda$):

$$\frac{\partial c'}{\partial x_2}\Big|_0 = -\frac{\partial c'}{\partial x_2}\Big|_\lambda \tag{3-13}$$

Inserting (3-13) into (3-12) gives:

$$c'(x_2) = C_w - C + \frac{V}{d}\left[\frac{x_2^3}{3\varepsilon} - \frac{x_2^4}{2\varepsilon^2} - \frac{x_2^2}{2}\right]\frac{\partial C}{\partial x_1} + \left[\frac{x_2^2}{2\varepsilon} - x_2\right]\left[\frac{\partial c'}{\partial x_2}\Big|_\lambda\right]$$

(3-14)

Integrating (3-14) with respect to x_2 over the aperture width gives:

$$\left.\frac{\partial c'}{\partial x_2}\right|_{\blacksquare} = \frac{6}{\blacksquare}\left(\blacksquare\right) - \frac{V\blacksquare}{10d}\frac{\partial C}{\partial x_1} \tag{3-15}$$

Substituting (3-15) into (3-14) gives the zero-mean solution:

$$c'(x_2) = (C_w - C)\left[1 - 6\frac{x_2^2}{\blacksquare^2} - 6\frac{x_2}{\blacksquare}\left[\left[\frac{x_2^3}{\blacksquare} - \frac{x_2^4}{2\blacksquare^2} - \frac{3}{5}x_2^2 - \frac{x_2}{10}\right]\right]\right]\frac{V}{d}\frac{\partial C}{\partial x_1} \tag{3-16}$$

Differentiating (3-16) with respect to the x_2 direction and substituting λ for x_2 gives the concentration gradient:

$$\frac{d}{\blacksquare}\left[\left.\frac{\partial c'}{\partial x_2}\right|_0\right] = \frac{12d}{\blacksquare^2}\left[C_w - C\right] - \frac{V}{5}\frac{\partial C}{\partial x_1} \tag{3-17}$$

multiplying both sides with v', and averaging along the x_2 direction gives the diffusive flux:

$$\overline{c'v'} = -\left[C_w - C\right]\left[\frac{V}{5} - \frac{V^2\blacksquare^2}{700d}\frac{\partial C}{\partial x_1}\right] \tag{3-18}$$

Differentiating (3-18), substituting it and (3-17) into (3-8), and assuming longitudinal diffusion is much smaller than dispersion, the transport equation for the mean concentration can be written as:

$$\frac{\partial C}{\partial t} = V^*\frac{\partial C}{\partial x_1} - D^*\frac{\partial^2 C}{\partial x_1^2} = K^*\left[C_w - C\right]$$

(3-19)

where the Taylor approximations for the mean velocity, dispersion, and dissolution rate coefficient for the mean transport equation are:

$$V^* = \frac{7}{5}V \qquad D^* = d + \frac{V^2 \Delta^2}{700d} \qquad K^* = \frac{12d}{\Delta^2} \tag{3-20}$$

These coefficients provide the means to predict the transport of a solute that is independent of scale. The dissolution rate coefficient, K^*, is a first-order reaction rate with units of inverse time.

3.3 Numerical Solution

To validate the analytical solution, the 2D transport equation (3-5) was solved numerically using an explicit finite difference scheme. The partial differential equations are replaced by a set of algebraic finite difference equations in terms of the dependent variable c. The solution to the resulting series of simultaneous equations gives the values of the concentration c at the grid points. The concentration derivative with respect to time is approximated by a forward difference:

$$\left.\frac{\partial c}{\partial t}\right|_{t=k\Delta t} = \frac{c_{i,j}^{k+1} - c_{i,j}^{k}}{\Delta t} \tag{3-21}$$

where k is the time step number and i and j are the grid indices in the x_1 and x_2 directions respectively. The concentration derivatives with resect to x_1 are approximated by central differences:

$$\left.\frac{\partial c}{\partial x_1}\right|_{x_1} = \frac{c^k_{i+1,j} - c^k_{i-1,j}}{2\Delta x_1} \tag{3-22}$$

Second-order concentration derivatives with respect to x_1 and x_2 are approximated by:

$$\left.\frac{\partial^2 c}{\partial x_1^2}\right|_{x_1} = \frac{c^k_{i+1,j} - 2c^k_{i,j} + c^k_{i-1,j}}{\Delta x_1^2} \qquad \left.\frac{\partial^2 c}{\partial x_2^2}\right|_{x_2} = \frac{c^k_{i,j+1} - 2c^k_{i,j} + c^k_{i,j-1}}{\Delta x_2^2} \tag{3-23}$$

Substituting the difference equations into (3-5) gives the explicit difference scheme for the transport equation:

$$c^{k+1}_{i,j} = c^k_{i,j} + \Delta t\left[\alpha\left(\frac{c^k_{i+1,j} - 2c^k_{i,j} + c^k_{i-1,j}}{\Delta x_1^2} + \frac{c^k_{i,j+1} - 2c^k_{i,j} + c^k_{i,j-1}}{\Delta x_2^2}\right) - v(j)\left(\frac{c^k_{i+1,j} - c^k_{i-1,j}}{2\Delta x_1}\right)\right] \tag{3-24}$$

This finite difference scheme is explicit because the equation at each location can be solved directly from the concentration field at the previous time step. This scheme was chosen due to its relatively low computational time requirements. However, the scheme is first-order accurate in time and is also unstable for large time steps. The grid size for the simulation is 50 nodes in the x_1 direction and 40 nodes in the x_2 direction. Figures 3-2 and 3-3 show that the solution is essentially independent of grid resolution above $n_i = 30$ and $n_j = 20$ because the difference between the concentrations is less than the grid resolution. The step sizes, Δx_1 and Δx_2, were calculated by dividing the length in a particular direction by the number of nodes in that direction. The time step Δt was calculated three different ways:

$$\Delta t = 0.025\frac{\Delta x_1^2}{d} \qquad \Delta t = 0.025\frac{\Delta x_2^2}{d} \qquad \Delta t = 0.033\frac{\Delta x_1}{V}$$

(3-25)

which corresponds to 2.5% of the time to diffuse across a node in the x_1 and x_2 directions and 3.3% of the time to advect across a node in the x_1 direction. These Δt's are based on a Courant-type approximation (Faires and Burden, 1996), but were not rigorously calculated. The Δt estimate with the smallest value was used as the time step in order to ensure stability. The simulation was run to steady state defined by the convergence to an asymptotic value of concentration. An example of the time evolution of concentration for a single location in the center of the flow is shown in Figure 3-4. After 1000 seconds the concentration solution has clearly reached an asymptotic value.

To further validate the numerical approach and results, the classic dispersion flow geometry described in Section 2.2 was calculated for comparison purposes. Figures 3-5 through 3-7 show the diffusive flux for Pe = 5000, 50 and 0.5, respectively. These Peclet numbers were chosen to represent advection-dominated, mixed, and diffusion-dominated flow regimes, respectively. These Peclet numbers also correspond to physically realistic regimes. For instance, a fracture with dimensions of 1000 mm in the x_1 direction and 1 mm in the x_2 direction, a constant molecular diffusion coefficient of 0.001 mm^2/s and a range of flow velocities from 0.0005 mm/s to 5 mm/s produces the Peclet numbers tested here. This value for the diffusion coefficient corresponds to typical values measured in the laboratory such as benzene at 20 °C (Wilke and Chang, 1955). Furthermore, Table 3-1 shows molecular diffusion coefficients for various ions in water at a constant temperature. For the low Peclet number results, the diffusive flux agrees extremely well

with the analytical solution. For Pe = 5000 there is not as close an agreement as the smaller Peclet numbers. This is expected since one of the major assumptions in the analysis is that diffusion dominates advection. Despite this assumption the agreement is still reasonable as shown in Figure 3-5.

Figures 3-8 through 3-10 show the mean concentration profile in the x_1 direction for the same Peclet numbers. The profile shows how the concentration is equal to the initial concentration near the inlet and goes to zero downstream of the inlet. The location in the longitudinal direction that the concentration goes to zero depends on the affect of advection. The concentration goes to zero closer to the inlet as the advection decreases. The gradual decrease in concentration is due to diffusion. Again, the agreement between the numerical simulation and the analytical result is excellent even for the Pe = 5000 case. From these comparisons we conclude that the numerical approach is an effective means of calculating the classical dispersion problem. The numerical approach will be applied to the current flow geometry in the next chapter.

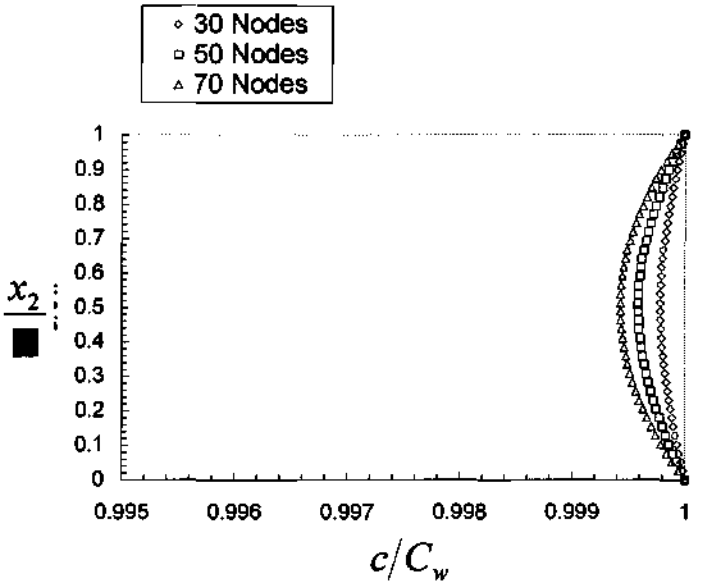

Figure 3-2 The mean concentration for three grid resolutions in the x_1 direction. The x_1 location corresponds to the end of the domain.

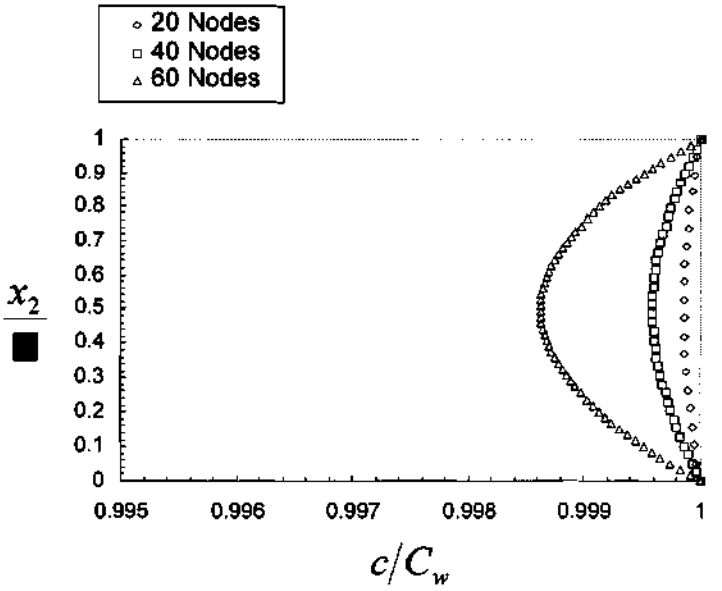

Figure 3-3 The concentration profiles for three grid resolutions in the x_2 direction. The x_1 location corresponds to the end of the domain.

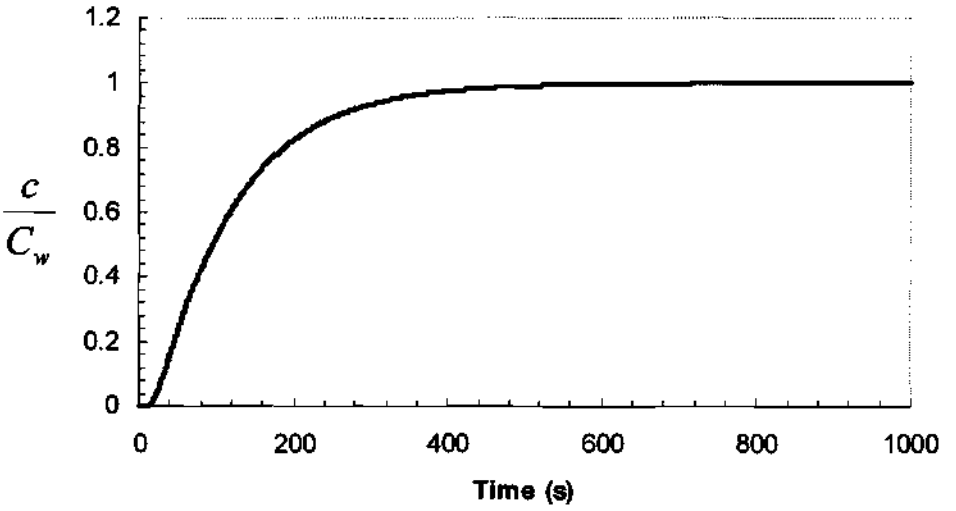

Figure 3-4 Concentration evolution at single point demonstrating convergence of steady state for Pe = 50.

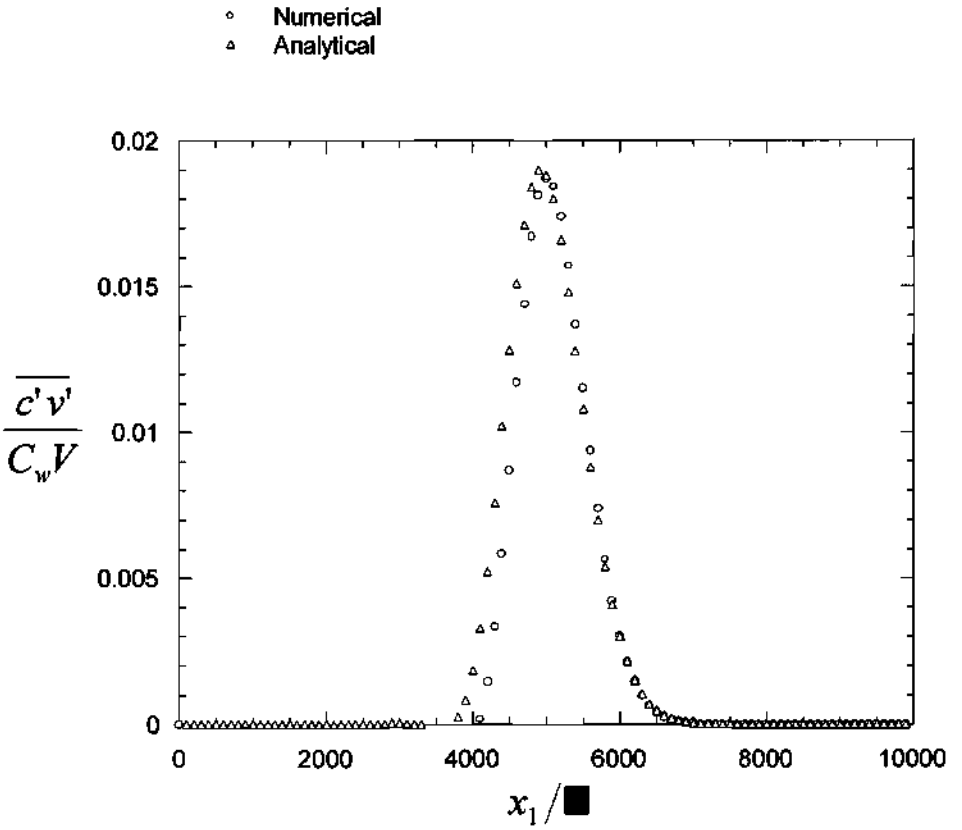

Figure 3-5 Diffusive flux for Pe = 5000.

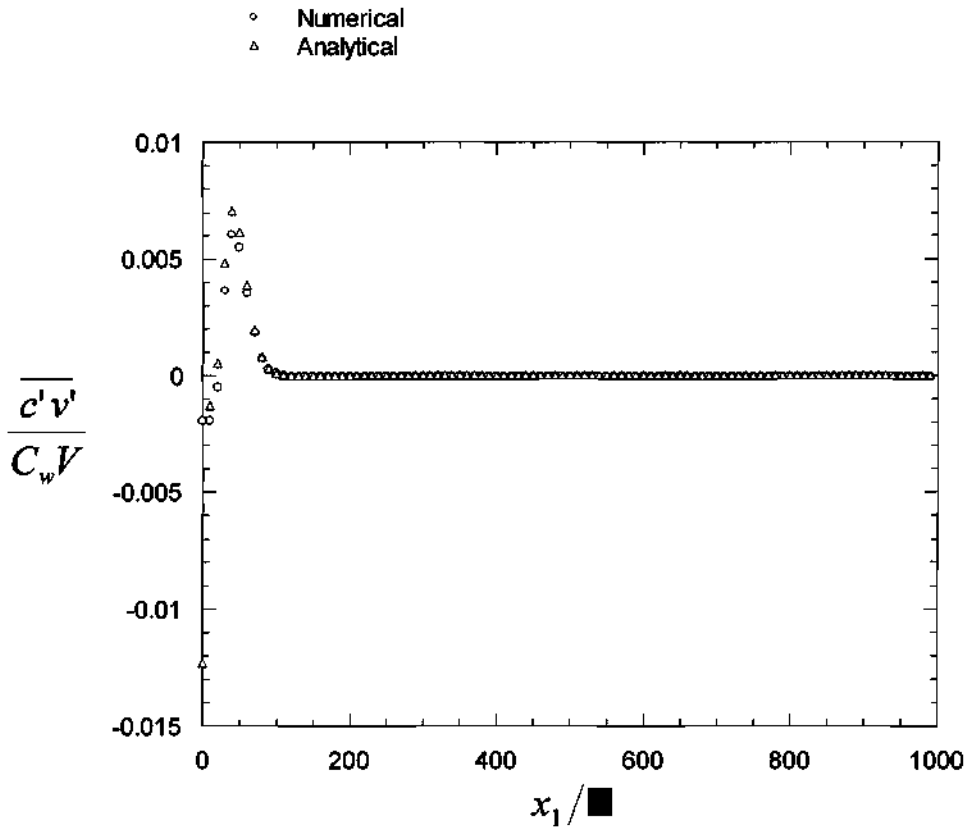

Figure 3-6 Diffusive flux for Pe = 50.

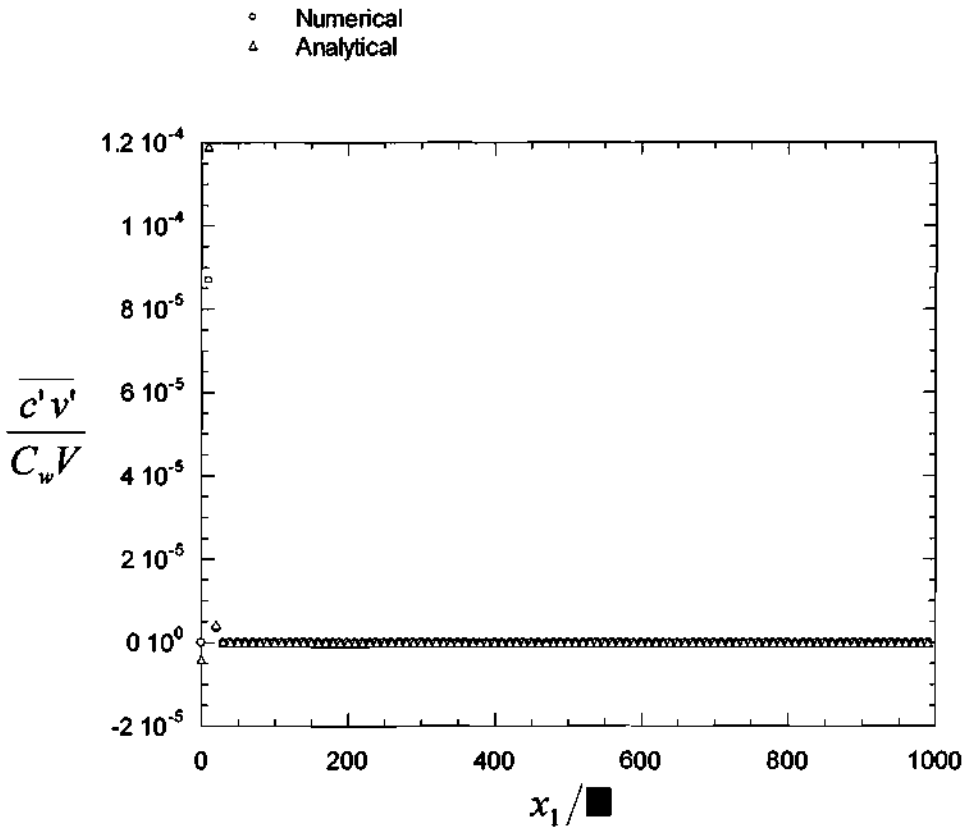

Figure 3-7 Diffusive flux for Pe = 0.5.

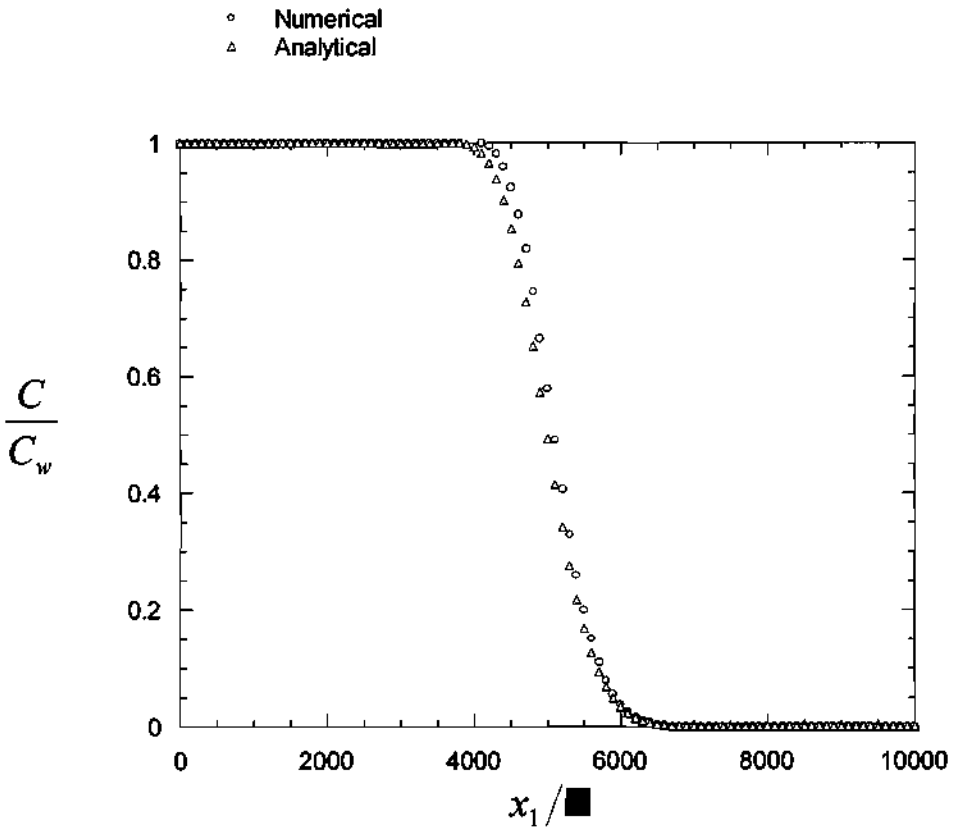

Figure 3-8 Mean concentration for Pe = 5000 at t* = 5000.

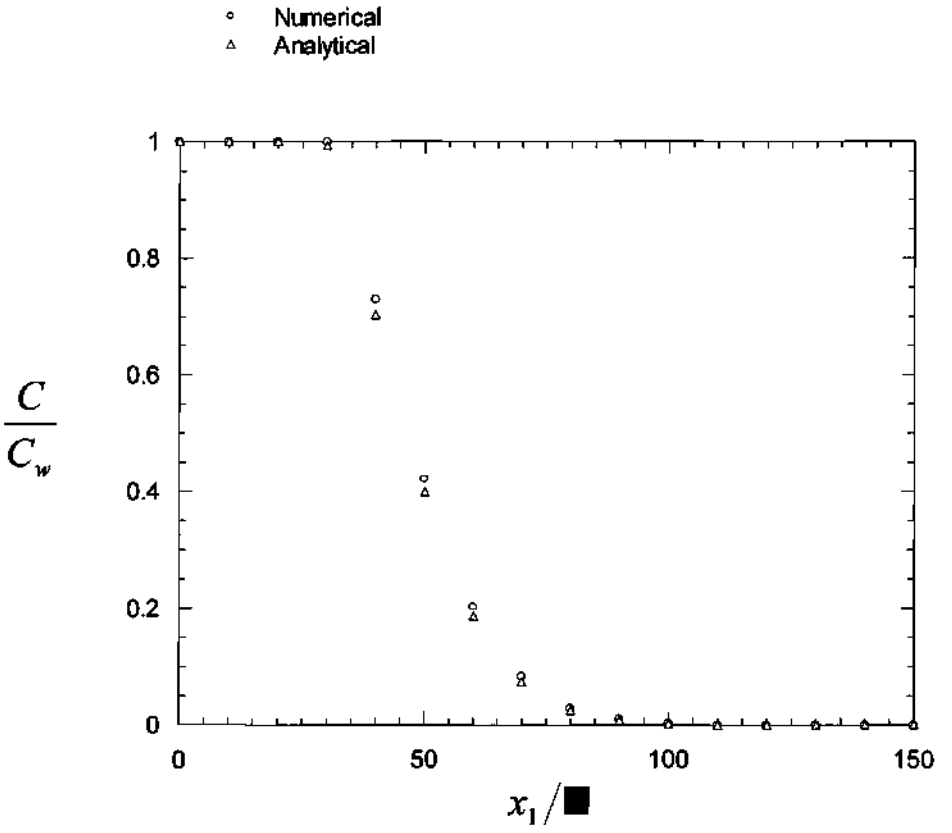

Figure 3-9 Mean concentration for Pe = 50 at t* = 50.

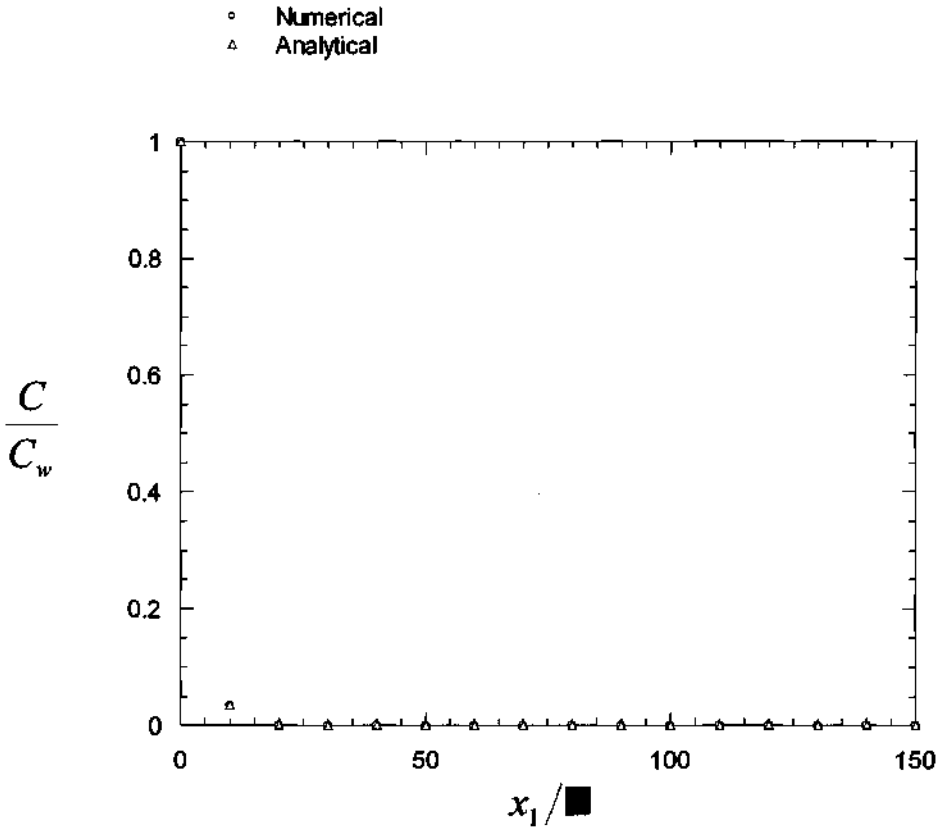

Figure 3-10 Mean concentration for Pe = 0.5 at t* = 0.5.

Table 3-1 Diffusion coefficients in water at 25°C (Li and Gregory, 1974)

Cations	
H^+	9.31×10^{-9} m²/sec
Na^+	1.33×10^{-9} m²/sec
K^+	1.96×10^{-9} m²/sec
Rb^+	2.06×10^{-9} m²/sec
Cs^+	2.07×10^{-9} m²/sec
Mg^{2+}	7.05×10^{-10} m²/sec
Ca^{2+}	7.93×10^{-10} m²/sec
Sr^{2-}	7.94×10^{-10} m²/sec
Ba^{2+}	8.48×10^{-10} m²/sec
Ra^{2+}	8.89×10^{-10} m²/sec
Mn^{2+}	6.88×10^{-10} m²/sec
Fe^{2+}	7.19×10^{-10} m²/sec
Cr^{3+}	5.94×10^{-10} m²/sec
Fe^{3+}	6.07×10^{-10} m²/sec
Anions	
OH^-	5.27×10^{-9} m²/sec
F^-	1.46×10^{-9} m²/sec
Cl^-	2.03×10^{-9} m²/sec
Br^-	2.01×10^{-9} m²/sec
HS^-	1.73×10^{-9} m²/sec
HCO_3^-	1.18×10^{-9} m²/sec
SO_4^{2-}	1.07×10^{-9} m²/sec
CO_3^{2-}	9.55×10^{-10} m²/sec

CHAPTER IV

RESULTS AND DISCUSSION

As described in the preceding chapter, an analytical solution for the dissolution rate coefficient was found for a 2D laminar shear flow between parallel plates with dissolution of solute from the walls. The analytical solution produced a mean velocity, dispersion coefficient, and dissolution rate coefficient that are independent of scale. In this chapter, the analytical expression is evaluated for a fracture for the Peclet numbers 5000, 50, and 0.5. Physically this corresponds to a constant molecular diffusion coefficient of 0.001 mm^2/s, a range of flow velocities from 0.0005 mm/s to 5 mm/s, and a gap width of 1mm. For the smaller Peclet number cases, the domain length was 1000■. For Pe = 5000 the domain was extended to 10000■ due to the relatively large velocity and advection. In addition, the numerical simulation described was run to steady state for the same flow parameters. The objective of this study was to compare the diffusive flux, concentration gradient in the transverse direction, and the mean concentration profiles in order to validate the analytical solution.

4.1 Mean Concentration

The analytical solution for the mean concentration follows:

$$\frac{\partial C}{\partial t} = V^* \frac{\partial C}{\partial x_1} - D^* \frac{\partial^2 C}{\partial x_1^2} = K^* (C_w - C) \tag{4-1}$$

where the Taylor approximations for the mean velocity, dispersion, and dissolution rate coefficient for the mean transport equation are:

$$V^* = \frac{7}{5} V \qquad D^* = d + \frac{V^2 \tau^2}{700 d} \qquad K^* = \frac{12 d}{\tau^2} \tag{4-2}$$

In steady state, (4-1) reduces to a second order differential equation with respect to x_1. The general solution to a second order differential equation of the form:

$$a \frac{\partial^2 y}{\partial x^2} + b \frac{\partial y}{\partial x} + c = 0 \tag{4-3}$$

is:

$$y = q_1 e^{m_1 x} + q_2 e^{m_2 x} \tag{4-4}$$

where m_1 and m_2 are the roots of the quadratic equation found by substituting this form into (4-3). The coefficients q_1 and q_2 are subsequently found from the boundary conditions.

The steady state reduction of (4-1) can be rearranged to:

$$D^* \frac{\partial^2 C}{\partial x_1^2} - V^* \frac{\partial C}{\partial x_1} - K^* (C - C_w) = 0 \tag{4-5}$$

defining a new variable $C^* = C - C_w$:

$$D^* \frac{\partial^2 C^*}{\partial x_1^2} - V^* \frac{\partial C^*}{\partial x_1} - K^* C^* = 0 \tag{4-6}$$

Comparing the general solution:

$$C^* = q_1 e^{m_1 x_1} + q_2 e^{m_2 x_1} \tag{4-7}$$

where:

$$m_1 = \frac{V^*}{2D^*} + \frac{1}{2}\sqrt{\left[\frac{V^*}{D^*}\right]^2 + 4\frac{K^*}{D^*}} \qquad m_2 = \frac{V^*}{2D^*} - \frac{1}{2}\sqrt{\left[\frac{V^*}{D^*}\right]^2 + 4\frac{K^*}{D^*}} \tag{4-8}$$

The boundary conditions in this case are:

$C^* = -C_w$ at $x_1 = 0$

$\frac{\partial C^*}{\partial x_1} = 0$ at $x_1 = L$

Applying these conditions yields:

$$c_1 = \frac{1}{\frac{m_1}{m_2} e^{L|m_1 - m_2|} - 1} \qquad c_2 = -1 - \frac{1}{\frac{m_1}{m_2} e^{[redacted]} - 1} \tag{4-9}$$

Figures 4-1, 4-2, and 4-3 show the comparisons between the analytical and numerical solutions. The results of the analytical solution show excellent agreement with the numerical solution. The mean concentration for the numerical and analytical solutions converges to 1.0 at the same x_1 position. The solutions are expected to converge to 1.0 because for a large time the fluid becomes uniform. This implies that the mass flux approaches to zero since the concentration gradients approach zero. The approach to uniform concentration slows with increasing *Pe* because advection moves the fluid much farther before diffusion from the walls homogenizes the field.

4.2 Diffusive Flux

The analytical solution (Equation 3-18) for the diffusive flux is:

$$\overline{c'v'} = -\left(C_w - C\right)\left(\frac{V}{5} - \frac{V^2\alpha^2}{700d}\right)\frac{\partial C}{\partial x_1} \tag{4-10}$$

The flux term is a good measure of the solution validity because it depends on both the mean velocity and dispersion coefficient. Figures 4-4, 4-5, and 4-6 show the comparisons between the analytical and numerical solutions. With the exception of Figure 4-4, the advection dominated regime, the flux for both the numerical and analytical solutions converge to zero very rapidly. The flux asymptotes to zero because at large time c' goes to zero as C approaches 1.0. The flux is negative because as a fluid particle moves toward the center of the flow, the concentration variation $c' < 0$ and the velocity variation $v' > 0$, therefore $\overline{c'v'} < 0$. The results vary with the Peclet number because the relative advection rate affects the mean concentration distribution as described above.

4.3 Concentration Gradient

The analytical solution (Equation 3-17) to the concentration gradient in the transverse direction is:

$$\frac{d}{\alpha}\left[\frac{\partial c'}{\partial x_2}\right]_0^{\alpha} = -\frac{12d}{\alpha^2}\left(C_w - C\right) - \frac{V}{5}\frac{\partial C}{\partial x_1} \tag{4-11}$$

The concentration gradient is a good measure of the solution validity because it depends on both the mean velocity and dissolution rate coefficient. Figures 4-7, 4-8, and 4-9

show the comparisons between the analytical and numerical solutions. The gradients for the numerical and analytical solutions converge to zero in a similar manner. The solution goes to zero because at large time c becomes uniform, hence there is no gradient of concentration. The gradient is positive because moving toward the center of flow from the upper wall, the change in c' and x_2 are both negative, therefore the concentration gradient is positive. The results vary with Peclet number, again, due to the increased relative advection.

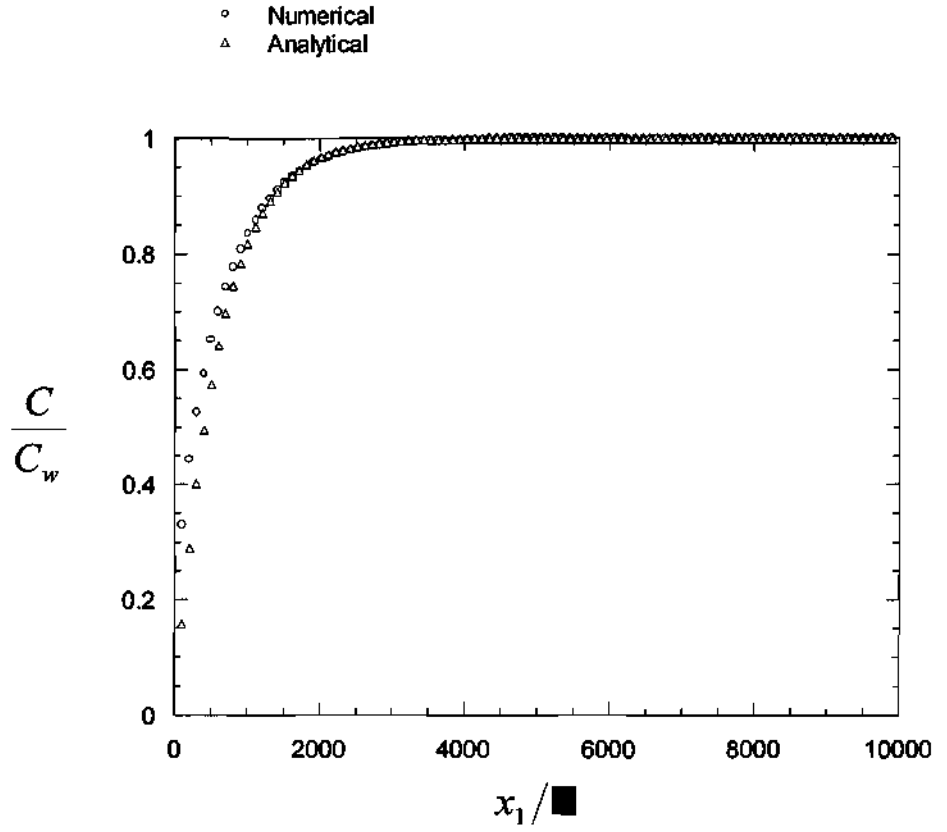

Figure 4-1 Mean concentration for Pe = 5000.

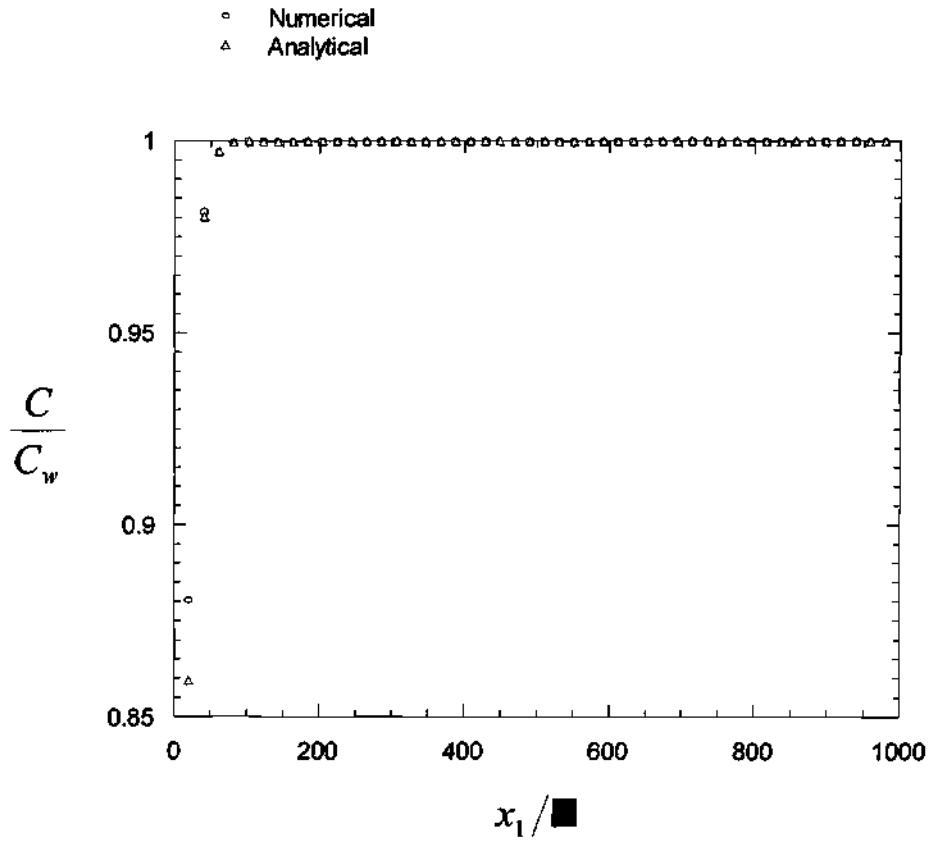

Figure 4-2 Mean concentration for Pe = 50.

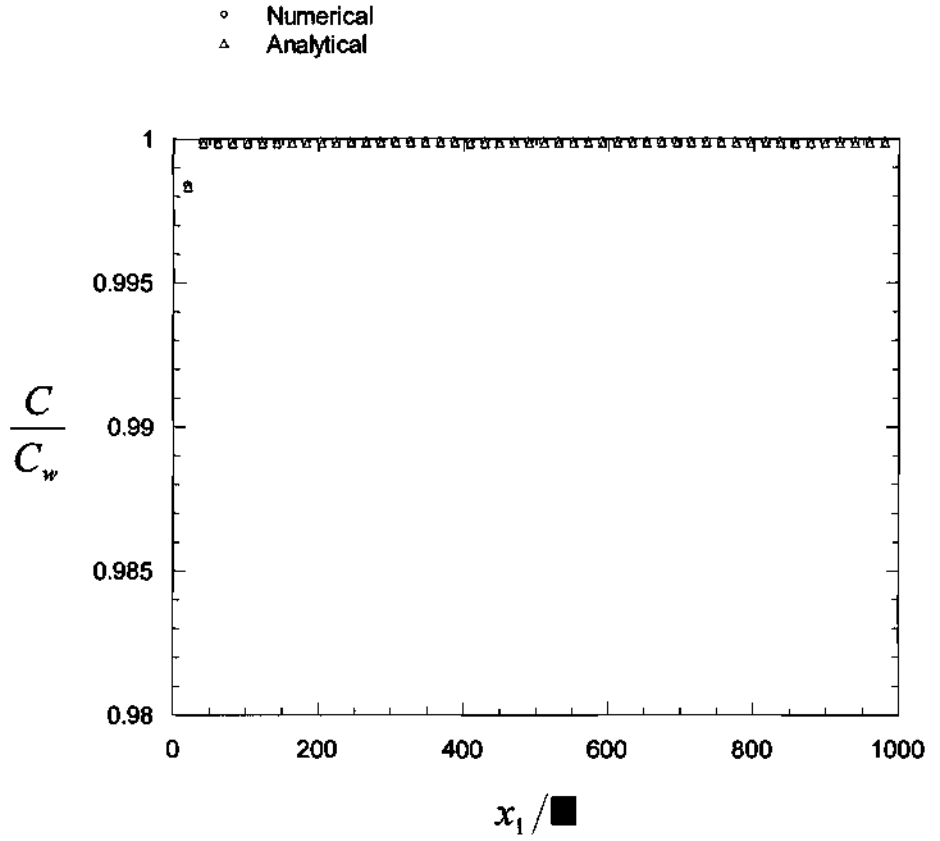

Figure 4-3 Mean concentration for Pe = 0.5.

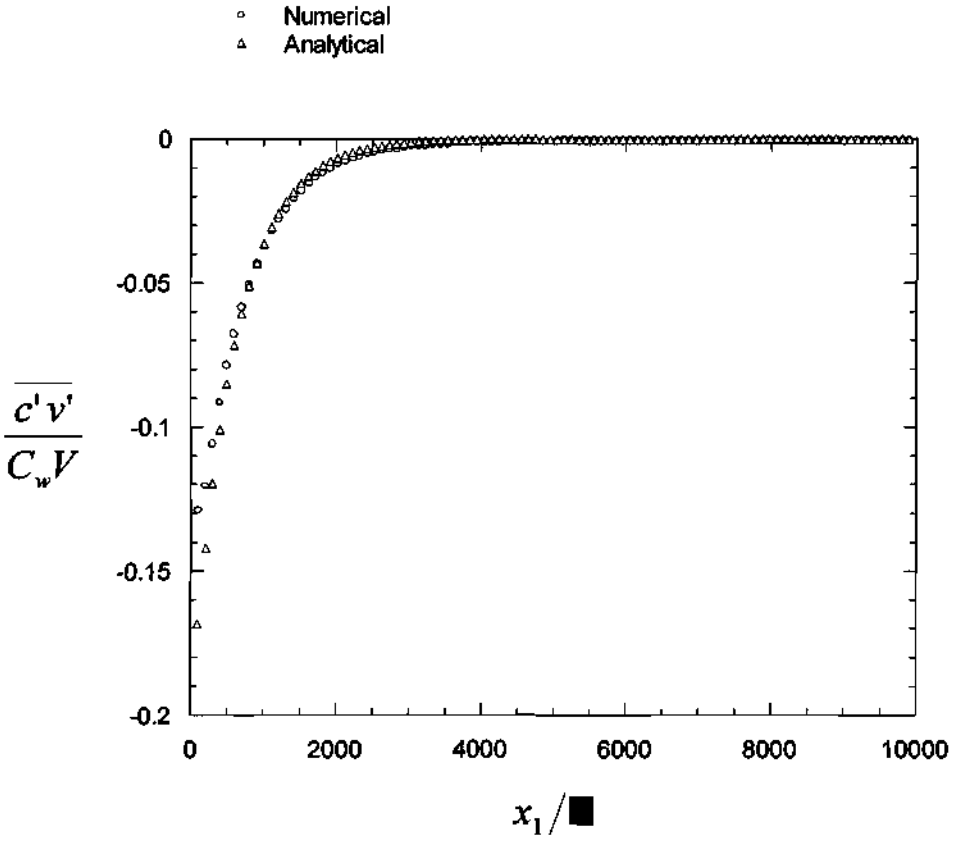

Figure 4-4 Diffusive flux for Pe = 5000.

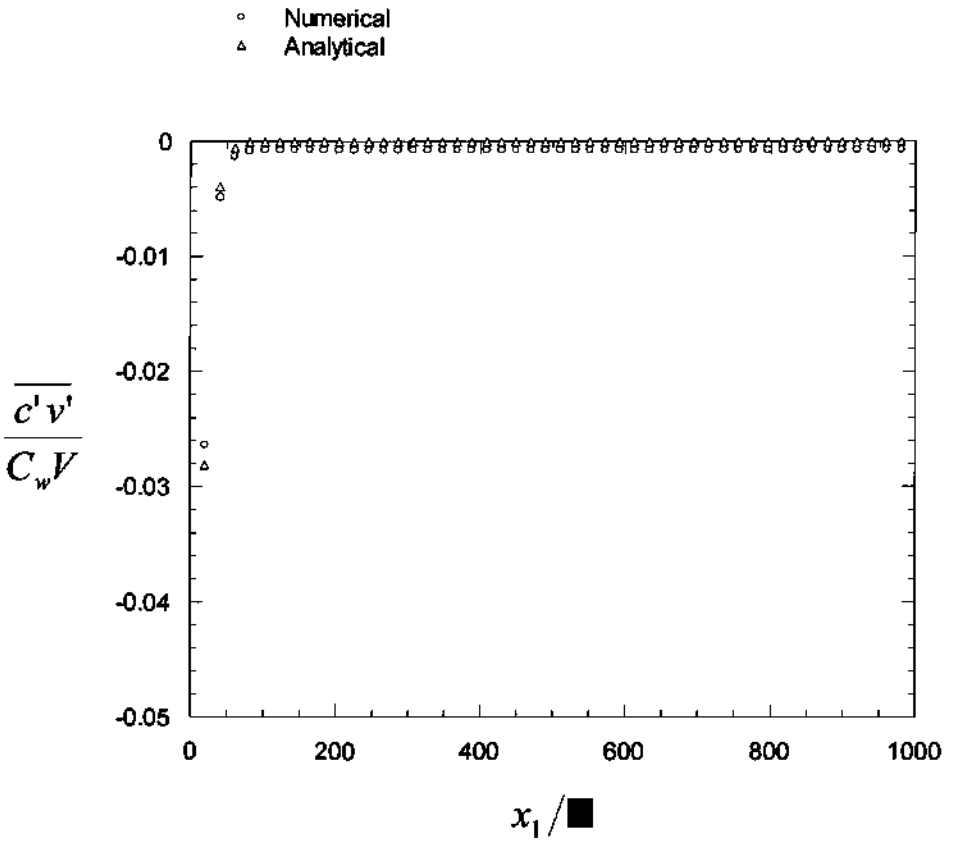

Figure 4-5 Diffusive flux for Pe = 50.

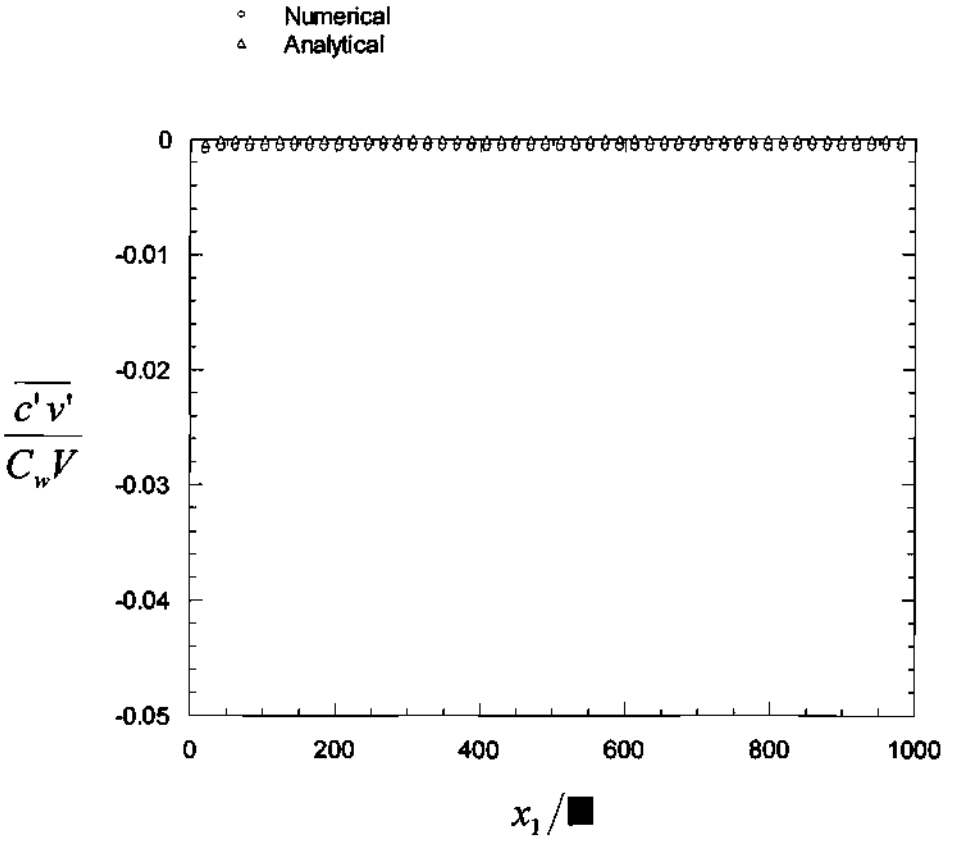

Figure 4-6 Diffusive flux for Pe = 0.5.

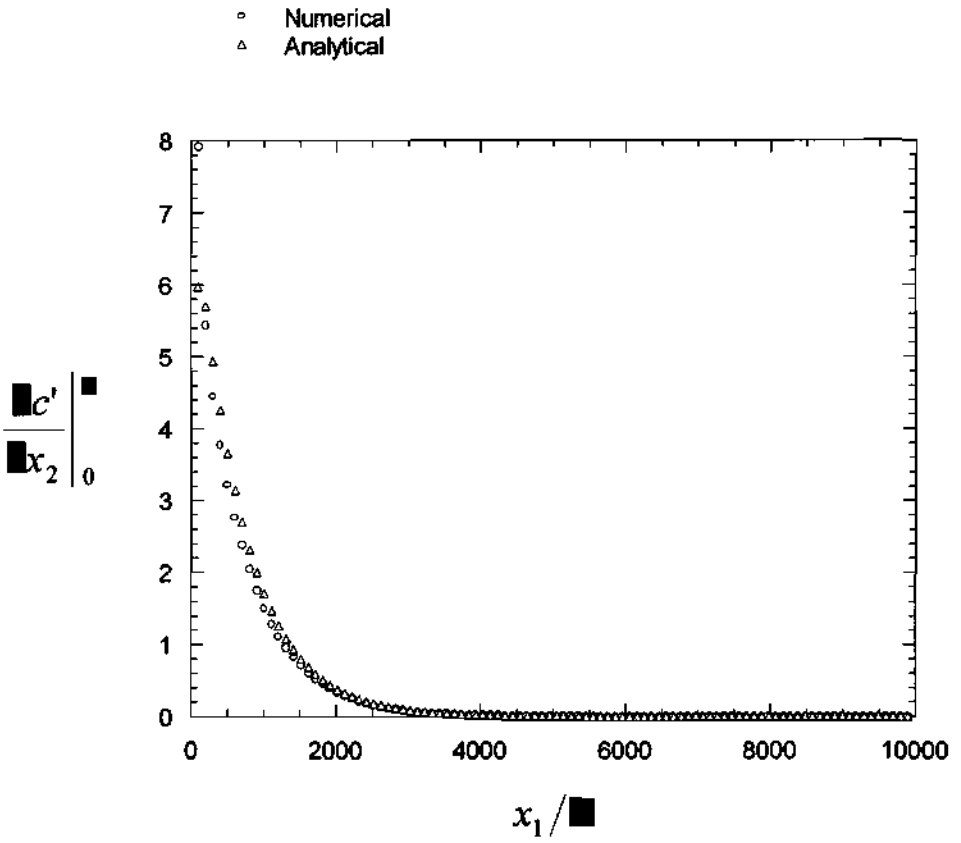

Figure 4-7 Concentration gradient for Pe = 5000 (gradient non-dimensionalized by C_w and ■).

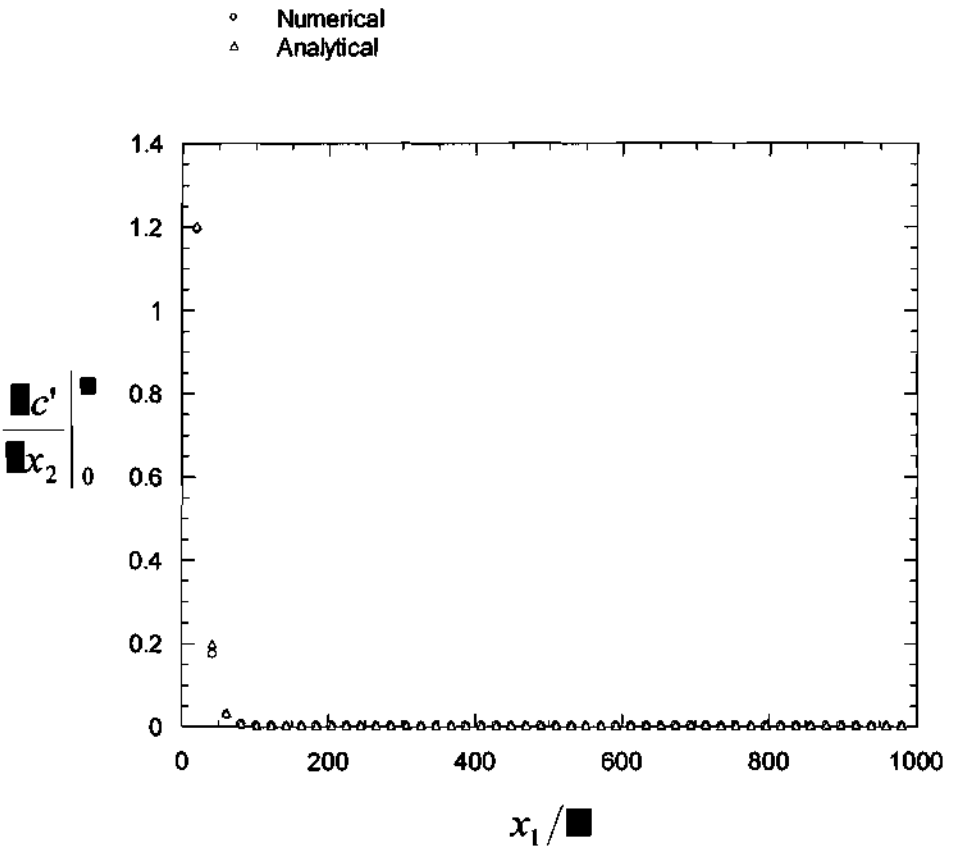

Figure 4-8 Concentration gradient for Pe = 50 (gradient non-dimensionalized by C_w and ■).

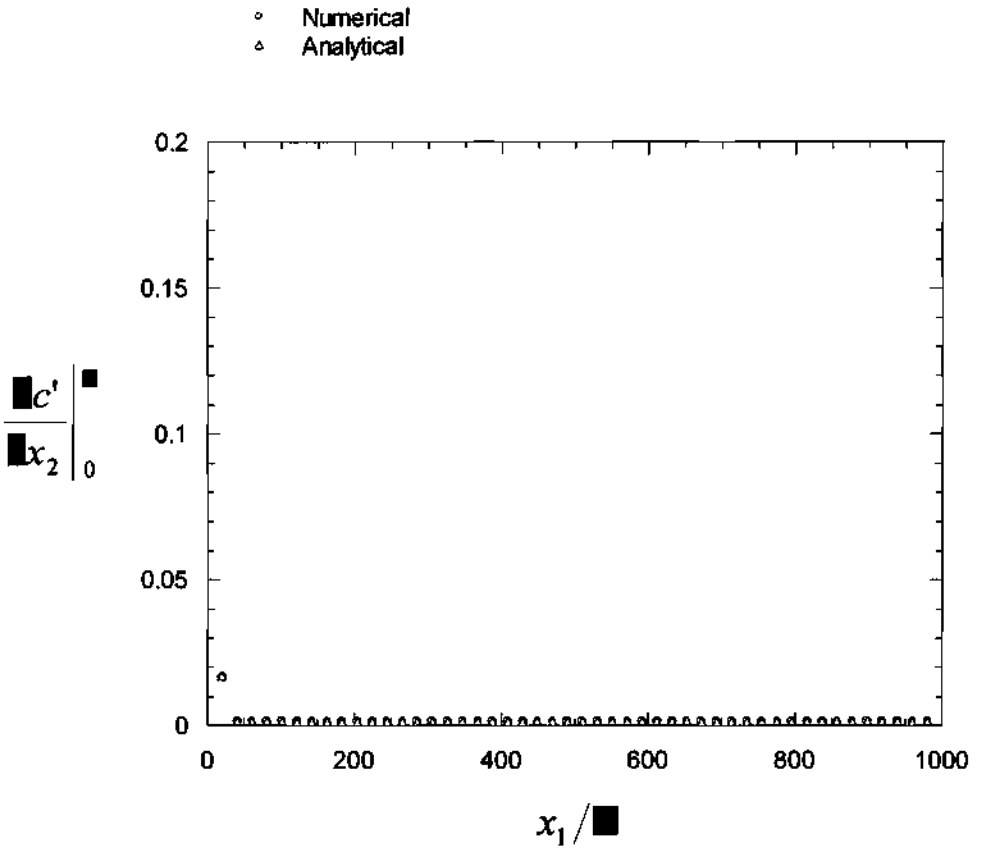

Figure 4-9 Concentration gradient for Pe = 0.5 (gradient non-dimensionalized by C_w and ■).

CHAPTER V

SUMMARY

In this study, an analytical dissolution rate coefficient that is independent of scale was developed in order to yield more realistic models for mass transfer in rock fractures. Following the analysis of Taylor (1953), a 2D laminar shear flow solution was found for the flow between parallel plates, where the boundaries were at a fixed location with a specified concentration. This idealized geometry simulates flow in a rock fracture with dissolving walls. The analytical solution yields the mean velocity, dispersion coefficient and dissolution rate coefficient, which are independent of scale and may be applied to NAPL and solid dissolution. To validate the analytical solution, the diffusive flux, concentration gradient in the transverse direction, and mean concentration were compared to the results of numerical simulations of the 2D advection-dispersion equation using a finite difference method.

In a range of Peclet numbers (0.5 to 5000) spanning the advection- and diffusion-dominated transport regimes, the results showed excellent agreement with the numerical solution. For the advection-dominated regime (Pe = 5000), the analytical solution is less accurate, which is consistent with the assumptions of the solution.

The solutions to the mean concentration converged to 1.0 because for a large time the fluid becomes uniform. This implies that the mass flux approaches to zero since the

concentration becomes uniform. The approach to uniform mean concentration C slows with increasing Peclet number because advection moves the fluid much farther before diffusion from the walls homogenizes the field. The flux asymptotes to zero because at large time the concentration variation c' goes to zero as C approaches 1.0. The flux is negative because as a fluid particle moves toward the center of the flow, the concentration variation c' is negative and the velocity variation v' is positive, therefore the diffusive flux $\overline{c'v'}$ is negative. The concentration gradient goes to zero because at large time c becomes uniform, hence there is no gradient of concentration.

This research can be extended to address more complex issues of interest to engineers and scientists working on rock fracture problems. For example, desorption of solutes from the fracture walls can be modeled similarly. However, the 2D transport equation would have to contain a retardation factor to account for sorption processes (Wels et al., 2000). In addition, the walls' position and concentration changing over time due to dissolution would lead to more complex flows that would require solving the Navier-Stokes equations along the wall boundaries. Furthermore, this study could also be applied to precipitation kinetics, which is simply the reverse of dissolution.

REFERENCES

Aris, R. 1956. On the dispersion of a solute in a fluid flowing through a tube. Proc. Roy. Soc. London A 252: 67-77.

Bekri, S., J.F. Thovert and P.M. Adler. 1997. Dissolution and deposition in fratures. Engineering Geology 48: 283-308.

Dijk, P. and B. Berkowitz. 1998. Precipitation and dissolution of reactive solutes in fractures. Water Resources Research 34(3): 457-470.

Dillard, L.A. and M.J. Blunt. 2000. Development of a pore network simulation model to study nonaqueous phase liquid dissolution. Water Resources Research 36(2): 439-454.

Faires, J.D. and R. Burden. 1998. Finite-Difference Methods for Parabolic Problems. *In* Numerical Methods. Brooks/Cole Publishing Company, Pacific Grove, CA, 481-482.

Fischer, H.B., E.J. List, R.C.Y. Koh, J. Imberger, and N.H. Brooks. 1979. Mixing in Inland and Coastal Waters, Academic, San Diego, Calif.

Holtta, P., M. Hakanen, A. Hautojarvi, J. Timonen and K. Vaatainen. 1996. The effects of matrix diffusion on radionuclide migration in rock column experiments. Journal of Contaminant Hydrology 21: 165-173.

Li, Y.H. and S. Gregory. 1974. Diffusion of ions in sea water and in deep-sea sediments. Geochemica et Cosmochemica Acta, 38: 703-714.

Morel, F.M.M. 1983. Solid Dissolution and Precipitation. *In* Principles of Aquatic Chemistry. John Wiley & Sons, Inc., New York, NY, 178-236.

Parker, B.L., R.W. Gillham and J.A. Cherry. 1994. Diffusive disappearance of immiscible phase organic liquids in fractured geologic media. Ground Water 32(5): 805-820.

Parsons, A.M., N.E. Olague and D.P. Gallegos. 1991. Conceptualization of a high-level nuclear waste repository site in unsaturated, fractured tuff. U.S. Nuclear Regulatory Commision, NUREG/CR-5495, Washington, D.C.

Taylor, G.I. 1953. Dispersion of soluble matter in solvent flowing slowly through a tube. Proc. Roy. Soc. London A 219: 186-203.

Weber, W.J. and F.A. DiGiano. 1996. Macrotransport Processes. *In* Process Dynamics in Environmental Systems. John Wiley & Sons, Inc., New York, NY, 97-146.

Wels, C., L. Smith and R. Beckie. 1997. The influence of surface sorption on dispersion in parallel plate fractures. Journal of Contaminant Hydrology 28: 95-114.

Wilke, C.R. and P.I.N. Chang. 1995. Correlation of diffusion coefficients in dilute solutions. A.I.Ch.E. Journal 1: 264-270.